# Endosomal sorting of Notch receptors through COMMD9-dependent pathways modulates Notch signaling

Haiying Li,[1] Yeon Koo,[2] Xicheng Mao,[1] Luis Sifuentes-Dominguez,[3] Lindsey L. Morris,[1] Da Jia,[1] Naoteru Miyata,[1] Rebecca A. Faulkner,[1] Jan M. van Deursen,[4,5] Marc Vooijs,[7] Daniel D. Billadeau,[5,6] Bart van de Sluis,[8] Ondine Cleaver,[2] and Ezra Burstein[1,2]

[1]Department of Internal Medicine, [2]Department of Molecular Biology, and [3]Department of Pediatrics, University of Texas Southwestern Medical Center, Dallas, TX 75390
[4]Department of Pediatric and Adolescent Medicine, [5]Department of Biochemistry and Molecular Biology, and [6]Department of Immunology, Mayo Clinic, Rochester, MN 55905
[7]Department of Radiotherapy (MAASTRO)/GROW-School for Developmental Biology and Oncology, Maastricht University, 6229 ER Maastricht, Netherlands
[8]Molecular Genetics Section - Department of Pediatrics, University of Groningen, University Medical Center Groningen, 9713 AV Groningen, Netherlands

Notch family members are transmembrane receptors that mediate essential developmental programs. Upon ligand binding, a proteolytic event releases the intracellular domain of Notch, which translocates to the nucleus to regulate gene transcription. In addition, Notch trafficking across the endolysosomal system is critical in its regulation. In this study we report that Notch recycling to the cell surface is dependent on the COMMD–CCDC22–CCDC93 (CCC) complex, a recently identified regulator of endosomal trafficking. Disruption in this system leads to intracellular accumulation of Notch2 and concomitant reduction in Notch signaling. Interestingly, among the 10 copper metabolism MURR1 domain containing (COMMD) family members that can associate with the CCC complex, only COMMD9 and its binding partner, COMMD5, have substantial effects on Notch. Furthermore, *Commd9* deletion in mice leads to embryonic lethality and complex cardiovascular alterations that bear hallmarks of Notch deficiency. Altogether, these studies highlight that the CCC complex controls Notch activation by modulating its intracellular trafficking and demonstrate cargo-specific effects for members of the COMMD protein family.

## Introduction

Copper metabolism MURR1 domain containing (COMMD) proteins are a group of highly conserved factors defined by the presence of a unique C-terminal homology domain (Burstein et al., 2005). Ten family members can be identified from mammals to unicellular protozoa (Maine and Burstein, 2007), but little is known about their cellular functions and the underlying reason for their conservation and diversification. Most of our understanding is centered on *COMMD1*, the first identified member of this family that was initially noted to be the site of a recessive mutation that results in copper toxicosis in a particular dog breed, the Bedlington terrier (van de Sluis et al., 2002).

The mechanism for the accumulation of copper in these animals was initially unclear; however, an interaction between COMMD1 and the copper transporter ATP7B was reported early on (Tao et al., 2003). Recently, we demonstrated that COMMD1 regulates the endosomal sorting of the copper transporter ATP7A, such that in the absence of COMMD1, ATP7A is trapped in endosomal vesicles and lacks copper-dependent trafficking to the trans-Golgi network and plasma membrane (Phillips-Krawczak et al., 2015). In addition to its control of ATP7A/7B trafficking, COMMD1 has been linked to the regulation of other transporters, including epithelial sodium channel, cystic fibrosis transmembrane conductance regulator, and sodium-potassium-chloride cotransporter 1 (Biasio et al., 2004; Drévillon et al., 2011; Smith et al., 2013). However, whether these other transporters are similarly regulated at the level of endosomal sorting remains to be examined. Furthermore, COMMD1 has also been linked to other pathways that are seemingly not connected to the endolysosomal system, including nuclear factor κB regulation (Maine et al., 2007; Starokadomskyy et al., 2013) and hypoxia adaptation (van de Sluis et al., 2010).

The role of COMMD1 in endosomal sorting is linked to its incorporation into a larger complex containing the coiled-coil proteins CCDC22 and CCDC93 (Phillips-Krawczak et al., 2015). This COMMD–CCDC22–CCDC93 (CCC) complex localizes to endosomes through interactions between CCDC22 and CCDC93 with FAM21 (Harbour et al., 2012; Freeman et al., 2014; Phillips-Krawczak et al., 2015), a component of the Wiskott-Aldrich syndrome protein and scar homolog (WASH) complex (Derivery et al., 2009; Gomez and Billadeau, 2009). WASH is a member of the Wiskott-Aldrich syndrome protein

Correspondence to Ezra Burstein: ezra.burstein@utsouthwestern.edu

Abbreviations used in this paper: CCC, COMMD–CCDC22–CCDC93; CCDC, coiled-coiled domain containing; COMMD, copper metabolism MURR1 domain containing; E, embryonic day; LC-MS/MS, liquid chromatography tandem mass spectrometry; MEF, mouse embryo fibroblast; qRT-PCR, quantitative RT-PCR; WASH, Wiskott-Aldrich syndrome protein and scar homolog.



The Rockefeller University Press $30.00
J. Cell Biol. Vol. 211 No. 3 605–617
www.jcb.org/cgi/doi/10.1083/jcb.201505108

family of actin nucleation-promoting factors (Rottner et al., 2010). Through its ability to recruit and activate the ubiquitously expressed Arp2/3 complex, WASH promotes endosomal actin deposition and is required for the maintenance of the architecture of the endolysomal system and to facilitate receptor trafficking (Derivery et al., 2009, 2012; Gomez and Billadeau, 2009; Jia et al., 2010; Gomez et al., 2012).

COMMD proteins are known to interact with each other through their COMM domains (Burstein et al., 2005); moreover, all COMMD family members have been shown to interact with the CCC complex component CCDC22 (Starokadomskyy et al., 2013). However, whether other COMMD proteins form distinct CCC entities and can mediate unique functions that distinguish them from COMMD1 has not been elucidated. At the present time, studies addressing functions of other COMMD proteins are scant and include roles in epithelial sodium channel regulation (Liu et al., 2013), regulation of cell proliferation and repair in kidney injury models (Devlin et al., 2003), effects on hepatocellular carcinoma (Zheng et al., 2012), and regulation of IκB protein degradation (Starokadomskyy et al., 2013).

In this study, we performed an extensive functional analysis of *COMMD9*, a COMMD family member that is frequently deleted in WAGR syndrome (MIM 194072), a congenital condition caused by a microdeletion and haploinsufficiency at 11p13 (Xu et al., 2008). We report that COMMD9 is incorporated into the CCC complex and plays a critical role in endosomal sorting of Notch family members. Upon ligand binding, Notch proteins undergo proteolytic cleavage to release the Notch intracellular domain, which in turn translocates to the nucleus and along with cofactors binds gene-promoter regions of chromatin to regulate gene expression (Kopan, 2012). Furthermore, extensive work in *Drosophila* and other models has uncovered that trafficking of Notch proteins through the endolysosomal system is critically important in regulating their activity (Wilkin et al., 2008; Fortini and Bilder, 2009; Kandachar and Roegiers, 2012; Troost et al., 2012). Here we describe that in the absence of COMMD9, Notch expression is reduced at the cell surface and Notch2 is missorted into cytosolic vesicles from where it can reach lysosomes, resulting in reduced Notch-dependent signaling. Furthermore, we show that *Commd9* is critically required during mammalian development and that it functions as part of a unique CCC complex.

## Results

### Identification of the COMMD9 interactome

To begin to understand what unique function COMMD9 might mediate, we used tandem affinity purification to define its protein interactome. To that end, COMMD9 was doubly tagged with a tandem HA tag in its N terminus and a short biotinylation sequence in its C terminus. The protein was immunopurified with an HA antibody first, and on elution, it was purified again using streptavidin resin. The final material, when resolved by SDS-PAGE and stained with silver nitrate, demonstrated several unique bands in addition to the purified bait (Fig. 1 A). These bands were excised and subjected to trypsin digestion for proteomic identification by liquid chromatography tandem mass spectrometry (LC/MS-MS). This analysis identified 37 interacting proteins with high confidence (Table S1). CCDC22, CCDC93, and COMMD5, components of a recently identified regulator of endosomal protein sorting (Starokadomskyy et al., 2013; Phillips-Krawczak et al., 2015), were found in this purification (Fig. 1 B). The Rab proteins RAB5C, RAB7A, and RAB11B, which are present in different endosomal subcompartments, were also found. In addition, several transmembrane surface proteins were also identified (Fig. 1 B). Among these proteins, Notch2 was identified through four peptides mapping to both the N-terminal extracellular portion of the receptor and its C-terminal tail. This receptor was of interest to us because of its important developmental roles (High and Epstein, 2008).

### COMMD9 interacts with Notch proteins

The interaction between COMMD9 and Notch2 was readily recapitulated by coimmunoprecipitation, which also detected that COMMD9 interacts with members of the CCC complex, as expected (Fig. 1 C). Furthermore, COMMD9 also coimmunoprecipitated Notch1, another family member (Fig. 1 D); in comparison, Notch3 was not coprecipitated to a significant degree (Fig. 1 E).

### COMMD9 and the CCC and retromer complexes regulate surface levels of Notch2

The CCC complex is a regulator of endosomal sorting events mediated by retromer and WASH, including the endosome-to-surface recycling of the copper transporter ATP7A (Phillips-Krawczak et al., 2015). With this in mind, we reasoned that COMMD9 might similarly regulate the recycling of Notch2 to the plasma membrane. To assess this possibility, we screened a series of Notch2 antibodies and cell lines to identify suitable reagents that allow immunofluorescence staining of the endogenous protein. Among different laboratory variants of HeLa cells, we identified a subline with high expression of Notch2 that is suitable for immunofluorescence staining. Next, we derived *COMMD9* knockout clones of this cell line using CRISPR/Cas9 gene editing technology using two separate guide RNA sequences targeting exon 1 of *COMMD9* (Fig. S1 A). All three clones had no detectable protein expression (Fig. 2 A), and genomic analysis demonstrated short deletions in the targeted region (Fig. S1, B and C). In these cells, we identified that the normal surface staining pattern of Notch2 was largely lost, and instead, this was replaced by prominent intracellular vesicular staining for Notch2 in all three clones (Fig. 2 B). Furthermore, although the overall Notch2 protein expression was only modestly decreased in these cells, surface protein biotinylation demonstrated a substantial reduction of Notch2 in this fraction (Fig. 2, C and D), consistent with the reduced plasma membrane staining pattern noted by immunofluorescence staining. In addition, we also examined the nature of the intracellular Notch2 accumulation seen in *COMMD9*-deficient cells. The intracellular Notch2 puncta in *COMMD9*-deficient cells partly colocalized with EEA1, and to a lesser extent with VPS35 (Fig. S2, A and B). Consistent with the notion that these puncta represent early endosomes, Rab5 colocalized with Notch2 in *COMMD9*-deficient cells, whereas the colocalization with the recycling endosome marker Rab11 was poor (Fig. S2 C).

Next, expression of COMMD9 was restored in two of the targeted clones to ensure that these observations were indeed specific to *COMMD9* targeting (Fig. 2 E). Surface biotinylation experiments demonstrated that the rescued lines had increased Notch2 levels at the cell surface (Fig. 2, F and G), indicating that this cellular phenotype is rescued by COMMD9 re-expression. Furthermore, silencing of CCDC93 or C16orf62 (two additional components of the CCC complex) also led to reduced plasma membrane staining for Notch2, a pattern also observed

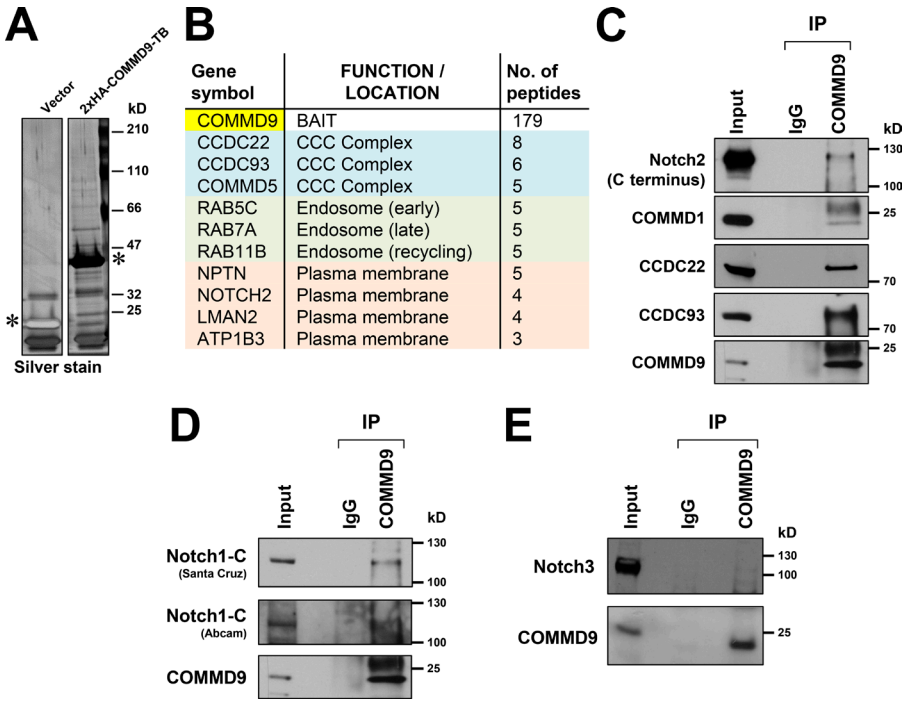


Figure 1. **Identification of COMMD9-interacting proteins.** (A) Tandem affinity purification of COMMD9 (HA and TB tagged) in HEK293 cells was followed by SDS-PAGE and silver staining. The location of the bait, or the control polypeptide expressed by the empty vector, is marked by an asterisk. Other coprecipitated bands are evident in the COMMD9 lane. Molecular mass markers (in kD) are noted. (B) Top hits identified by LC/MS-MS. (C) Confirmation of the endogenous interaction between COMMD9 and Notch2. COMMD9 was immunoprecipitated with specific antibodies, and the precipitates were immunoblotted for Notch2 (using an antibody that is specific for its C-terminal region) and other proteins as indicated. Molecular mass markers (in kD) are noted. (D and E) COMMD9 interacts with Notch1 but not Notch3. Endogenous COMMD9 was immunoprecipitated and associated proteins were immunoblotted for Notch1 (D, two individual antibodies that are specific for Notch1 C terminus) and Notch3 (E). Molecular mass markers (in kD) are noted.

on silencing of VPS35 (Fig. S3, A and B), a subunit of the retromer complex which is important for WASH recruitment and function (Harbour et al., 2012; Jia et al., 2012). Altogether, these findings indicate that the absence of COMMD9 and associated factors results in the accumulation of Notch2 in the early endosomal compartment.

## COMMD9 is required for optimal Notch signaling

Next we assessed the effects of COMMD9 on Notch-dependent gene expression. *COMMD9*-deficient HeLa cell clones displayed decreased basal expression of several Notch-dependent genes, but this HeLa subline proved to be poorly responsive to

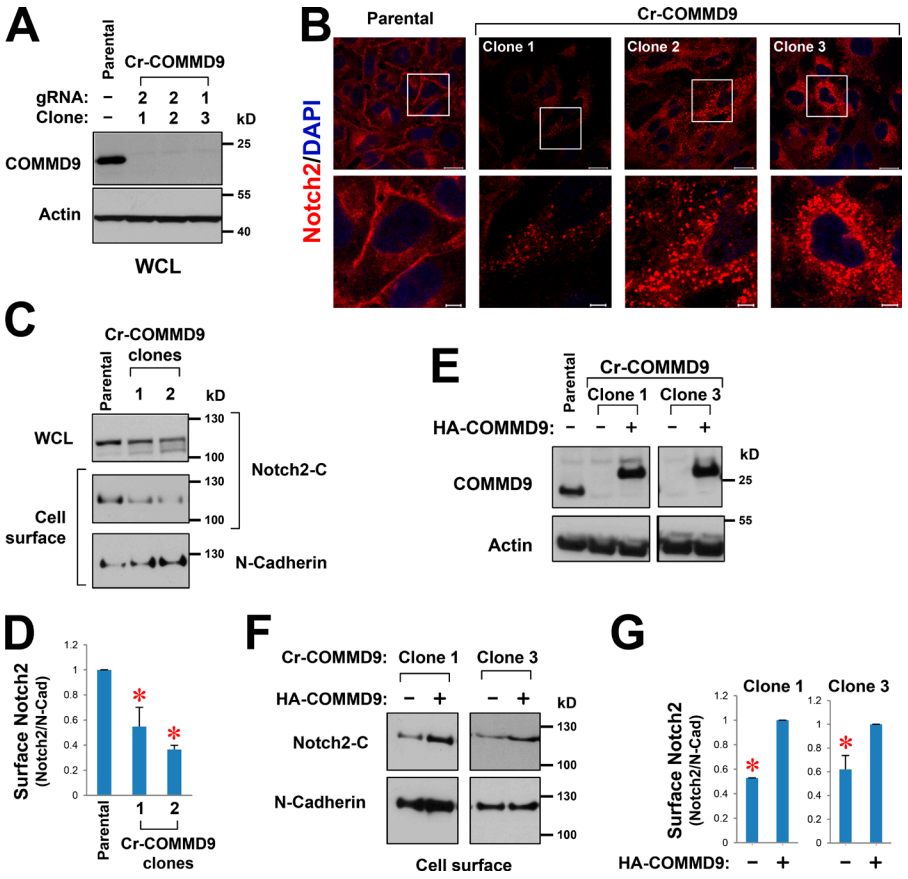


Figure 2. **COMMD9 regulates the surface localization of Notch2.** (A) Generation of COMMD9-deleted HeLa cells with CRISPR/Cas9 technology (Cr-COMMD9). Western blots for COMMD9 are shown in three clones derived using two different guide RNA sequences (gRNA). Molecular mass markers (kD) are noted. (B) Localization of Notch2 in parental HeLa cells and in Cr-COMMD9 clones was assessed by immunofluorescence staining. Bars: (top) 20 µm; (bottom) 5 µm. (C and D) Surface Notch2 was also assessed by biotinylation, precipitation, and immunoblotting as described in the Materials and methods section (C). The immunoblots for N-cadherin serve as loading controls. Molecular mass markers (in kD) are noted. Semiquantitation was performed by densitometry analysis, and the averages of three independent iterations are presented (D). Error bars represent the SEM. *, $P < 0.05$. (E) HA-COMMD9 was reintroduced using a lentiviral vector resulting in rescued expression of COMMD9 in clones 1 and 3, as shown here by immunoblotting. Molecular mass markers (in kD) are noted. (F and G) Notch2 surface expression was assessed by biotinylation and immunoblotting (E). Molecular mass markers (in kD) are noted. Semiquantitation by densitometry analysis and the averages of three independent iterations are presented (G). Error bars represent the SEM. *, $P < 0.05$.

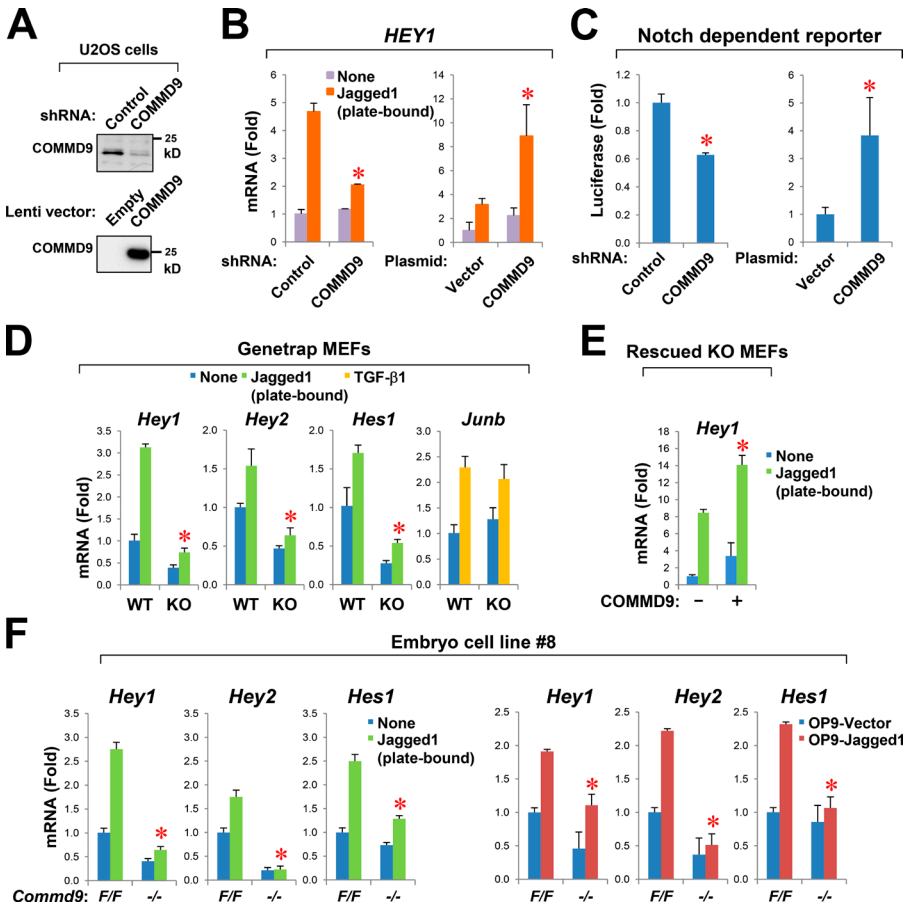


Figure 3. **COMMD9 deficiency impairs Notch-dependent gene expression.** (A) U2OS cells stably deficient in COMMD9 or expressing HA-COMMD9 were generated using lentiviral vectors. COMMD9 Western blots with molecular mass markers (in kD) are shown. (B) U2OS cells shown in Fig. 3 A were stimulated with Jagged1 (plate bound), and the induction of *HEY1* mRNA was determined by qRT-PCR. Triplicate samples were averaged, and error bars represent the SEM. *, $P < 0.05$. (C) The same cells shown in Fig. 3 A were transfected with a Notch-responsive luciferase reporter. Luciferase activity was determined and normalized against the control conditions. Triplicate samples were averaged. Error bars represent the SEM. *, $P < 0.05$. (D) Immortalized MEFs obtained from wild-type (WT) or COMMD9-deficient (KO) littermate embryos were used. Cells were stimulated with Jagged1 (plate bound) or TGF-β (soluble), and the induction of Notch-responsive genes (*Hey1*, *Hey2*, and *Hes1*) or TGF-β responsive genes (*Junb*) was assessed by qRT-PCR. Triplicate samples were averaged. Error bars represent the SEM. *, $P < 0.05$. (E) Furthermore, COMMD9 expression was rescued in the KO line using a lentivirus, and the responsiveness of this control line was examined and compared against an empty vector control. Triplicate samples were averaged. Error bars represent the SEM. *, $P < 0.05$. (F) MEFs derived from an embryo with a conditional *Commd9* allele (F/F) were used to derive *Commd9*-deficient cells (−/−). These cells were stimulated with plate-bound Jagged1 (left) or cell-bound Jagged1 (right) and the induction of Notch responsive genes (*Hey1*, *Hey2*, and *Hes1*) was monitored by qRT-PCR. Triplicate samples were averaged. Error bars represent the SEM. *, $P < 0.05$.

stimulation with exogenous Jagged1 ligand (unpublished data). Therefore, we used alternative models to investigate this question. First, U2OS cells with stable silencing or stable overexpression of COMMD9 were used (Fig. 3 A). Using Jagged1 as ligand for Notch stimulation, we noted that COMMD9 silencing led to reduced induction of *HEY1*, a Notch target gene, whereas overexpression of COMMD9 had the opposite effect (Fig. 3 B). Furthermore, these cells were transfected with a Notch-responsive luciferase reporter containing a promoter with multimerized RBPj binding elements. Here we observed that the effects of COMMD9 expression on the Notch reporter were concordant with the observed effects on *HEY1* expression (Fig. 3 C), consistent with the notion that endogenous *HEY1* gene expression was indeed affected through a Notch-dependent event.

For further analysis, we used mouse embryo fibroblasts (MEFs) derived from a gene trap *Commd9*-deficient model, where a gene trap cassette was inserted between exons 5 and 6 of the mouse *Commd9* gene (Fig. S4 A). This targeted allele is in effect a complete knockout because Commd9 protein expression in mutant MEFs is undetectable (Fig. S4 B). *Commd9*-deficient MEFs from this gene trap model demonstrated substantial reductions in Jagged1-mediated induction of Notch target genes, such as *Hey1*, *Hey2*, and *Hes1*, whereas TGF-β1 responses were unaffected (Fig. 3 D). Furthermore, re-expression of Commd9 in these MEFs (Fig. S4 C) restored *Hey1* expression in this cell model (Fig. 3 E). Finally, we tested a second gene inactivation model that relies on the introduction of LoxP sites flanking exon 3 of the mouse *Commd9* gene (Fig. S4 D). MEF lines were derived from two embryos, and isogenic pairs lacking Commd9 expression were generated in culture by transient expression of Cre recombinase (Fig. S4 E). In agreement with previous observations, *Commd9* deficiency was associated with blunted activation of Notch target genes. This was true in response to plate-bound recombinant Jagged1, or when OP9 cells that stably express Jagged1 were used as a source of ligand (Fig. 3 F). Altogether, these findings indicate that COMMD9 is required for optimal activation of Notch-dependent gene expression, in agreement with the role of this protein in maintaining surface expression of Notch2.

## COMMD9 prevents the lysosomal degradation of Notch

Inactivation of retromer is frequently associated with missorting of endosomal protein cargoes to lysosomes, resulting in protein degradation (Steinberg et al., 2013). We noted a modest reduction of Notch2 in HeLa cells (Fig. 2 C) and assessed this phenomenon in other cell models. In this regard, we found that COMMD9 silencing in HEK 293 cells led to more notable reduction in Notch2 protein expression (Fig. 4 A). Unlike Notch2, silencing of COMMD9 had little impact on Jagged1 expression (Fig. 4 B). A similar phenomenon was noted for Notch1 and Notch2 in *Commd9*-deficient fibroblasts (Fig. 4 C), and this reduction was also noted in the cell surface fraction (Fig. 4 D). Importantly, Bafilomycin A1, an inhibitor of lysosomal acidification and protease activity, restored Notch2 expression in MEFs (Fig. 4 E). Altogether, these data are consistent with the notion that COMMD9 deficiency results in missorting of Notch

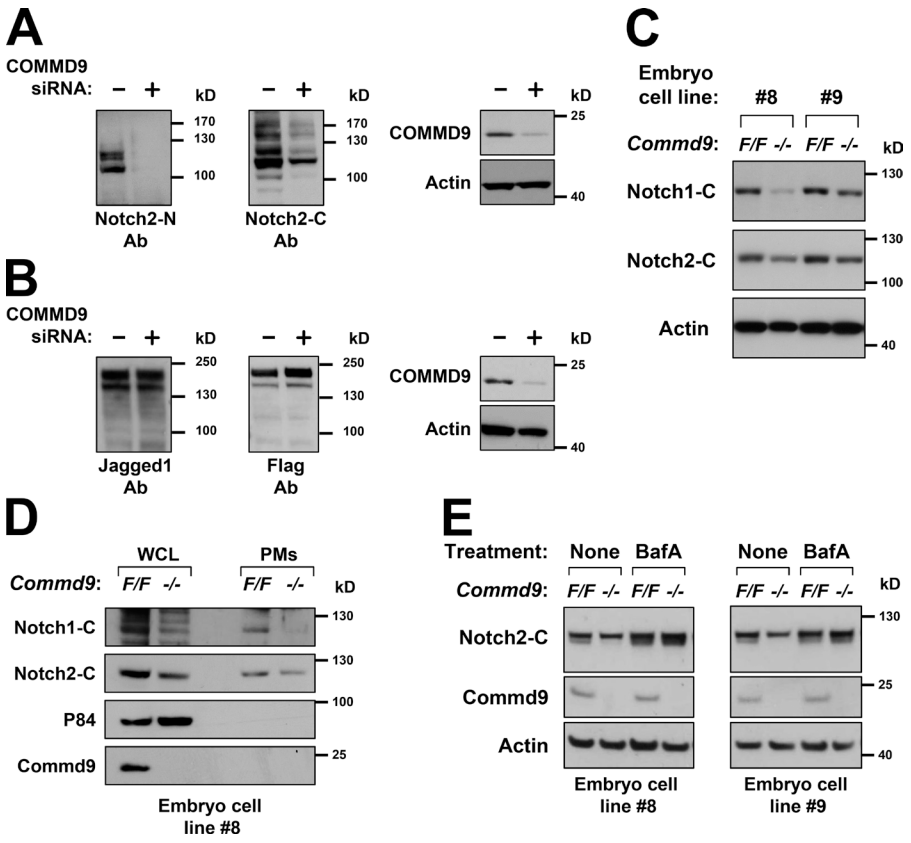


Figure 4. **COMMD9 deficiency leads to lysosomal degradation of Notch.** (A) HEK293 cells were transfected with a Notch2 expression vector; siRNA was used to concurrently silence COMMD9 expression. Notch2 expression was monitored using antibodies that recognize the extracellular domain (Notch2-N) or an intracellular epitope (Notch2-C). Molecular mass markers (in kD) are shown. (B) HEK293 cells were transfected with a Jagged1 expression vector; siRNA was used to concurrently silence COMMD9 expression. Jagged1 expression was evaluated using Jagged1 or FLAG antibodies. Molecular mass markers (in kD) are shown. (C) Levels of Notch1 and Notch2 expression in two *Commd9*-deleted cell lines (−/−) and their isogenic controls (F/F) were determined by immunoblotting. Molecular mass markers (in kD) are shown. (D) Using *Commd9* F/F and −/− MEFs, total Notch1 and Notch2 levels (whole-cell lysates [WCLs]) were determined in by immunoblotting (left). In addition, surface levels of both proteins (plasma membrane [PM]) were also determined by biotinylation and immunoblotting (right). Molecular mass markers (in kD) are shown. (E) The reduced expression of Notch2 shown in Fig. 4 C is rescued by Bafilomycin A1 (BafA) treatment, an inhibitor of endolysosomal acidification that impairs lysosomal proteases. Molecular mass markers (in kD) are shown.

proteins through the endolysosomal system, leading to their lysosomal degradation.

### Commd9 deficiency leads to abnormalities in cardiovascular development

In view of the aforementioned findings, and the important roles of Notch during embryogenesis (High and Epstein, 2008), we suspected that *Commd9* deficiency in mice could impair several developmental processes, including in the cardiovascular system. First, we observed that gene trap targeting of the *Commd9* locus was not viable at birth, and timed pregnancies indicated that the expected Mendelian rate was last observed at embryonic day (E) 10.5 (Fig. 5 A). At this stage, *Commd9*-deficient embryos displayed neural edema (Fig. 5 B), which was followed a day later by hemorrhages, starting in the head of the embryo and soon after observed throughout the body (Fig. 5 B, and C). Several other morphologic changes were noted, most notably in the cardiovascular system. Hypoplasia of the heart was a universal finding at E10.5 and beyond (Fig. 5 D), with foci of focal wall necrosis and pericardial bleeding noted by E11.5 (Fig. S4 F). Furthermore, mutant embryos displayed several vascular changes, including focal narrowing of the dorsal aortas (Fig. 5 E). Whole-mount immunohistochemistry staining for the endothelial marker Pecam1 revealed additional alterations in cranial blood vessels, particularly a dramatic reduction in truncal vessels connected to the distal capillary networks (Fig. S4 G). Further analysis with markers of arterial (Cx40) and venous (Apj) vessels revealed normal arterial structures but substantial changes in venous vasculature formation, with ectatic dilations noted in the embryo's head (Fig. S4 H). To assess if these changes were at least in part related to altered Notch signaling, we isolated heart mRNA from somite-matched embryos at E10.5. Indeed, a reduction in *Hey1* and *Hey2* mRNA expression in the heart was noted (Fig. 5 F), in line with the findings made in MEFs derived from this mouse strain (Fig. 3).

Interestingly, germline targeting in the *Commd9* floxed mouse recapitulated the embryonic lethality noted in the gene trap model (Fig. S4 I). However, endothelial (Tie2-Cre), myocardial (Nkx2.5-Cre), and smooth muscle (Sm22-Cre) targeting were all viable and did not recapitulate the embryonic lethal phenotype observed with whole-body deficiency (Fig. S4 I). Therefore, we concluded that the embryonic lethality we observed resulted from alterations in more than one discrete cell lineage.

### COMMD9 forms preferential complexes with COMMD5 and COMMD10

*Commd1* deficiency in mice has been shown to result in embryonic lethality (van de Sluis et al., 2007), with a phenotype that is earlier to that observed in the *Commd9*-mutant embryos studied here. Therefore, despite the similarities between these proteins, they serve nonredundant developmental functions that cannot be compensated by other COMMD proteins. To try to understand the potential basis for the specific effects noted for COMMD9 deficiency, we examined whether COMMD9 exists in a complex that is distinguishable from COMMD1. A side-by-side comparison of endogenous COMMD proteins associating with COMMD9 and COMMD1 indicated that both proteins coimmunoprecipitated with each other and result in similar recovery of several COMMD proteins, such as COMMD2, COMMD4, COMMD6, and COMMD8 (Fig. S5 A). However, COMMD5 and COMMD10 bound preferentially to COMMD9 over COMMD1. This suggested that COMMD9 and COMMD1 might coexist in overlapping but not identical complexes, and in

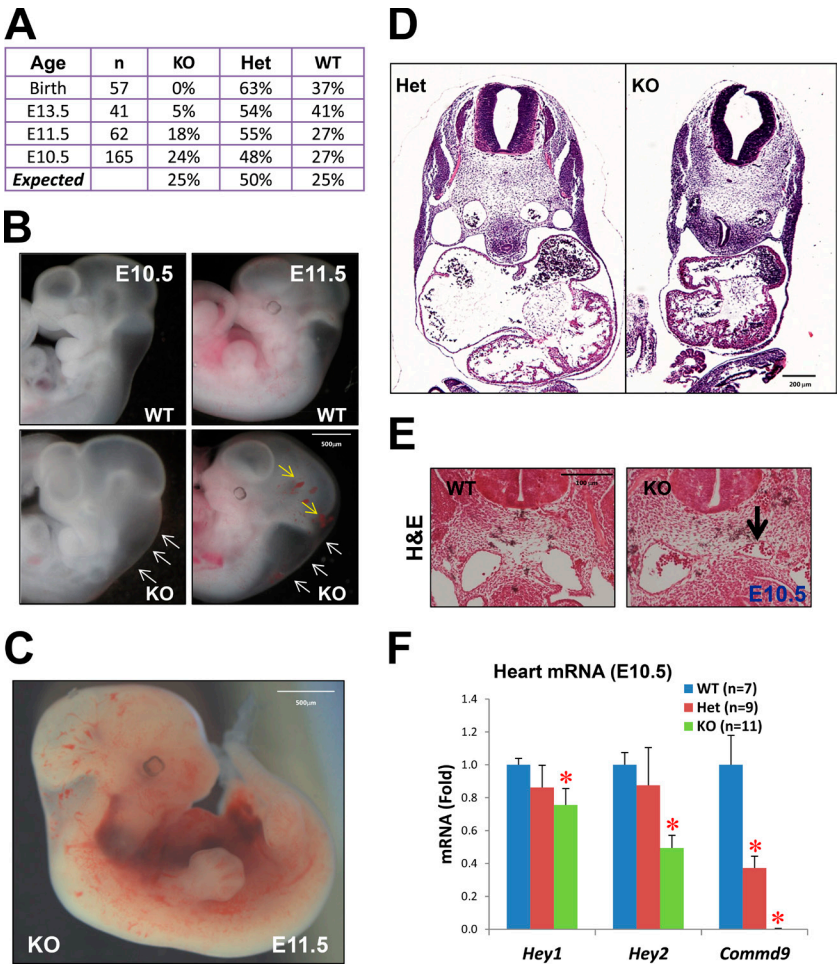


Figure 5. **COMMD9 deficiency leads to embryonic lethality and complex cardiovascular abnormalities.** (A) Genotyping results at different developmental stages demonstrate that *Commd9*-deficient mice (gene trap knockout [KO] model) are not viable at birth. Expected Mendelian rates are seen at E10.5. (B) KO embryos display neural tube edema (white arrows), seen by E10.5 (left). This is followed by punctate hemorrhages (yellow arrows), seen at E11.5 (right). WT, wild type. Bar, 500 µm. (C) KO embryos eventually developed widespread hemorrhages that are apparent by E11.5 and at later stages. Bar, 500 µm. (D) Cross-sectional histologic analysis demonstrated small hypoplastic hearts in all KO embryos. Bar, 200 µm. (E) Areas of unilateral narrowing of the dorsal aorta were commonly seen in mutant embryos (arrow). Bar, 100 µm. (F) Hearts were isolated from somite-matched E10.5 embryos. RNA was extracted from these organs, and qRT-PCR was used to determine the relative level of expression of two Notch target genes (*Hey1* and *Hey2*) and *Commd9*.

agreement with this, different ratios of COMMD9 and COMMD1 recovery were noted in each immunoprecipitation (Fig. S5 A).

In an additional analysis, five COMMD proteins were immunoprecipitated, demonstrating once again that COMMD9 was best immunoprecipitated by COMMD5 and COMMD10 (Fig. S5 B). Furthermore, COMMD5 was also more abundant in COMMD9 and COMMD10 immunoprecipitations, and the equivalent observation was made regarding COM MD10 (Fig. S5 B). In contrast, COMMD4 and COMMD6 only coimmunoprecipitated minimal amounts of COMMD5, COMMD9, and COMMD10. Corresponding to these interactions, COMMD9 and COMMD5 were found to colocalize in cytosolic puncta (Fig. 6 A). Altogether, these observations suggested that COMMD5, COMMD9, and COMMD10 form preferential complexes.

Finally, we examined whether key COMMD complexes observed here form through direct protein-protein interactions or are mediated indirectly through other factors present in cells. To that end, COMMD proteins were expressed recombinantly in *Escherichia coli*, and their ability to form complexes was assessed by coprecipitation. This analysis indicated that COMMD9 can bind directly to COMMD5, in agreement with the coimmunoprecipitation from cell lysates (Fig. 6 B). Interestingly, in this in vitro system, COMMD1 was able to bind to both COMMD5 and COMMD6, suggesting that additional cellular mechanisms might regulate the preferential in vivo binding of COMMD5 to COMMD9.

### COMMD9 and COMMD5 are preferentially involved in Notch regulation

Further examination indicated that loss of COMMD9 expression did not affect COMMD5 or COMMD10 expression in HeLa cells (Fig. 7 A) but abrogated their interactions with the CCC complex subunit CCDC22 (Fig. 7 B). In contrast, binding of CCDC22 with COMMD4, COMMD6, and COMMD8 was unaffected in these cells. Therefore, COMMD5 and COMMD10 are incorporated into the CCC complex in a COMMD9-dependent manner.

Next we examined the possibility that COMMD9-containing complexes are specifically involved in Notch2 regulation. To examine this, all 10 COMMD genes were individually silenced, and their effects on Notch2 expression were examined by immunoblotting. Only COMMD9 and COMMD5 silencing led to reduced Notch2 levels (Fig. 7 C). In agreement with this result, recombinant COMMD5-containing complexes were able to bind in vitro with an immunopurified C-terminal Notch2 polypeptide (Fig. 7 D). In contrast, COMMD1–COMMD6 complexes were unable to bind to Notch2. Collectively, these data suggest that COMMD9 forms unique COMMD heterocomplexes in cells that are required for the trafficking of Notch receptors.

## Discussion

This study sheds light into a previously unappreciated role for COMMD9 in vesicular sorting and the delivery of Notch

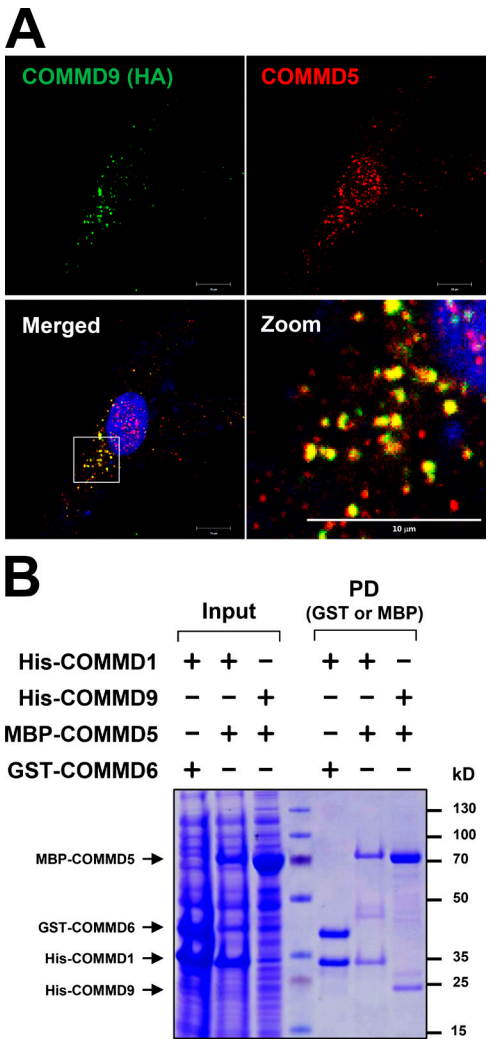


Figure 6. **COMMD9 interacts and colocalizes with COMMD5.** (A) Colocalization of COMMD9 and COMMD5 was evaluated in HeLa cells after CRISPR-mediated deletion and rescue of COMMD9 expression (Fig. 2 D; HA tagged, clone 3). Immunofluorescence staining for COMMD9 (HA) and COMMD5 was followed by confocal microscopy imaging. Bar, 10 µm. (B) In vitro binding between the indicated recombinant COMMD proteins. The indicated combinations of COMMD proteins were expressed in *E. coli* as described in the Materials and methods section. After lysis, one of the proteins (fused to the GST or MBP tag) was precipitated, and the presence of the partner COMMD protein was assessed by Coomassie blue staining. Molecular mass markers (in kD) are shown.

proteins to the cell surface. Absent COMMD9, Notch is mislocalized in intracellular early endosomes, and the response to Notch ligands is substantially attenuated. Furthermore, our studies indicate that Notch is not only mislocalized but also undergoes lysosomal degradation. Interestingly, we found that similar phenotypes are observed in cells deficient in CCC components CCDC93 and C16orf62 and the retromer subunit VPS35. This latter complex, which is critically important for the endosomal recycling of a large number of receptors (Seaman et al., 2013), has not been previously linked to Notch trafficking (Steinberg et al., 2013).

The observation that COMMD9-dependent effects on Notch trafficking can dramatically affect signaling is in line with a large body of literature that demonstrates that trafficking through the endolysosomal system is an evolutionarily conserved mechanism to regulate Notch activity (Baron, 2012; Kandachar and Roegiers, 2012). Notch is constantly endocytosed (McGill et al., 2009), and the signaling outcome arising from this internalized pool of Notch is carefully controlled by several factors. On the one hand, the protein Numb is a conserved inhibitor of the pathway that acts at this level (Cotton et al., 2013; Couturier et al., 2013, 2014; Reichardt and Knoblich, 2013). This factor interacts with components of the AP-2 complex and prevents endosome-to-plasma membrane recycling of Notch; in addition, Numb also promotes the lysosomal degradation of the receptor (McGill et al., 2009). In contrast, Deltex, an E3 ligase, has been shown to promote Notch signaling in a ligand-independent manner (Sakata et al., 2004; Wilkin et al., 2008; Hori et al., 2011, 2012; Troost et al., 2012). Acting in concert with the homotypic fusion and protein sorting complex and Rab7, Deltex promotes the trafficking of Notch to late endosomes. Interestingly, in this pathway, the localization of Notch is restricted to the limiting membrane of late endosomes, preventing the entry of the receptors into the multivesicular body. From this location, a ligand-independent cleavage event is thought to occur, resulting in pathway activation. Countering Deltex are HECT domain–containing ligases, such as Itch in mammals and Suppressor of Deltex in *Drosophila* (Wilkin et al., 2004; Chastagner et al., 2006), which promote the entry of Notch into the multivesicular body, resulting in its degradation.

Another intriguing observation made here is that the CCC complex, previously shown to regulate retromer/WASH-dependent endosomal trafficking, can have distinct configurations dictated by the incorporation of specific COMMD protein complexes. We show that COMMD5 and COMMD10 interact preferentially with COMMD9 and depend on this protein for their interaction with the CCC complex. The data further suggest that COMMD9–COMMD5 complexes are particularly important for Notch trafficking and can bind with the cytoplasmic tail of Notch2 in vitro. This raises the possibility that distinct CCC subcomplexes are generated to regulate specific cargoes and that perhaps COMMD proteins assist in cargo selection in this pathway.

In addition, it is reasonable to speculate that COMMD9 is likely to regulate many more receptors besides Notch. The identification of additional COMMD9-regulated cargoes will require proteome-wide analyses, such as those recently used to uncover retromer-regulated cargoes (Steinberg et al., 2013). This information would likely provide key insights that will be important to understand the developmental phenotypes resulting from *Commd9* deficiency. Our analysis identified several vascular and cardiac alterations, but the phenotype could not be ascribed entirely to the deficiency of a singular Notch receptor. For example, Notch1 deficiency has more prominent effects on arterial fate decisions (Lawson et al., 2001; Fischer et al., 2004; Gridley, 2010) rather than the phenotype in the venous vasculature observed here. Isolated *Notch2* deficiency is embryonically lethal at about the same stage as *Commd9* deficiency and is also associated with cardiac hypoplasia (Hamada et al., 1999; McCright et al., 2006), but only a small percentage of these mutant embryos exhibit neural and abdominal hemorrhages (Wang et al., 2012), as we routinely saw in *Commd9*-deficient embryos. Although *Notch3* deficiency is viable, combined *Notch2/Notch3* recapitulated more aspects of the phenotype of *Commd9*-deficient embryos. For example, concurrent deficiency of these factors results in frequent obstructions of the dorsal aortas and also leads to frequent cerebral and abdominal hemorrhages, as we saw here (Wang et al., 2012). However,

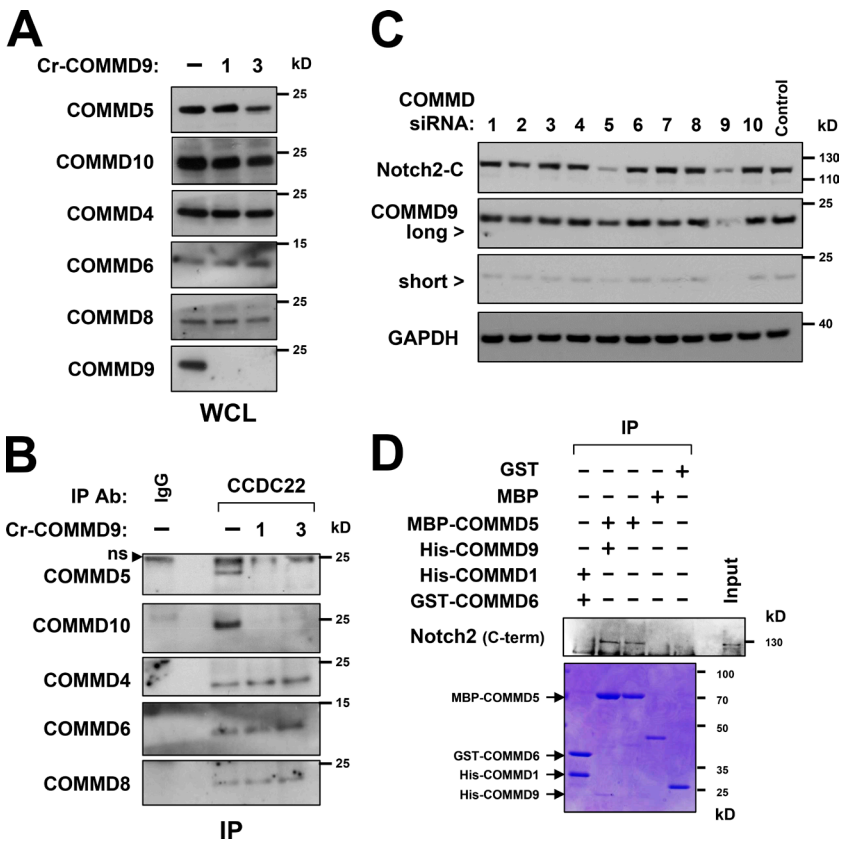


Figure 7. **COMMD9 and its partner COMMD5 regulate Notch2.** (A and B) The effects of COMMD9 deficiency on COMMD5 and COMMD10 interactions with the CCC complex were evaluated in two CRISPR clones. Endogenous input levels for several COMMD proteins were not substantially affected (A). In contrast, COMMD5 and COMMD10 interactions with the CCC complex subunit CCDC22 were lost in COMMD9-deficient cells. COMMD4, COMMD6, and COMMD8 were unaffected (B). Molecular mass markers (in kD) are shown. (C) In HEK 293T cells, each individual *COMMD* gene was silenced using siRNA transfection. Deficiency of either COMMD5 or COMMD9 led to reduced Notch2 expression. All other siRNA treatments did not affect this receptor. Molecular mass markers (in kD) are shown. (D) In vitro binding between an immunopurified Notch2 C-terminal polypeptide and recombinant COMMD complexes was evaluated by coprecipitation. Only COMMD5-containing complexes bound to Notch2. Molecular mass markers (in kD) are shown.

this phenotype in *Notch2/Notch3*-deficient embryos is largely driven by smooth muscle–dependent signals; in contrast, smooth muscle deletion of *Commd9* did not recapitulate the embryonic lethality. Altogether, our interpretation is that the developmental phenotypes in *Commd9*-deficient embryos are likely the result of alterations in additional receptors. In this regard, the fact that *COMMD9* is frequently included in the genomic interval deleted in WAGR syndrome highlights the biomedical importance of understanding these events. Patients with WAGR are affected by a high risk for Wilms' tumors and have several congenital anomalies, including aniridia, genitourinary abnormalities, intellectual disability, and frequent cardiac anomalies (Fischbach et al., 2005). We examined our heterozygote mice for any of these phenotypes and found no overt pathology, but cooperation between *COMMD9* and other genes may be relevant to the human condition.

In summary, this study identifies that COMMD9, acting in concert with the CCC and retromer complexes, regulates the endosomal sorting of Notch and its delivery to the cell surface. This constitutes a regulatory step in the Notch pathway that has not been previously appreciated. Future studies are likely to uncover that members of the COMMD protein family play similarly critical roles in the endosomal sorting of other important cell-surface receptors.

## Materials and methods

### Mouse strains

Mice were housed in conventional facilities and fed a standard diet. All animal procedures were approved by the institutional animal care and use committee. Gene-trapped *Commd9* mice were derived by the Transgenic Animal Model Core facility at The University of Michigan through blastocyst injection using an embryonic stem cell line (AQ0362) obtained from the Sanger Institute Gene Trap Resource (stock number 017754-UCD). The nature of the genomic targeting was confirmed by Southern blotting. Animals were genotyped by PCR using the following primers: 5′-TGCATGCCATAGAGCCCACTTGT-3′, 5′-TAGCAGCAGCCCCTCCATCACACT-3′, and 5′-GGGCTACC GGCTAAAACTTGAGAC-3′. This amplification yields a 530-bp product for the wild-type allele and a 771-bp product for the targeted allele. Mice with the conditional *Commd9* allele (*Commd9*$^{F/F}$), which contains LoxP sites flanking exon 3 of the *Commd9* gene, were generated by the Transgenic and Knockout Core at Mayo Clinic through blastocyst injection using an embryonic stem cell line (EPD0136_6_D10) obtained from The Knockout Mouse Project. Animals were genotyped by PCR using the following primers: 5′-AAGGTGGAAACACATAGCCAG-3′ and 5′-TTACTAGGCAACCCTGCATTG-3′. This amplification yields a 297-bp product for the wild-type allele and a 489-bp product for the targeted allele. Sox2-Cre transgenic mice are available from the Jackson Laboratory. This mouse strain contains a transgenic construct consisting of the promoter of the *Sox2* gene, which drives expression of Cre in the epiblast as early as E6.5 (Hayashi et al., 2002). The Nkx2.5-Cre mouse strain was provided by E. Olson (University of Texas Southwestern, Dallas, TX). This mouse contains a transgene consisting of a 2.5-kb fragment encompassing the promoter and cardiac enhancer of the *Nkx2-5* gene, which drives expression of Cre in the myocardium (McFadden et al., 2005). The Tie2-Cre mouse was provided by M. Yanagisawa (University of Texas Southwestern, Dallas, TX). This mouse contains a transgene consisting of the endothelial-specific promoter/enhancer of the *Tek (Tie2)* gene, which drives expression of Cre in endothelial cells (Kisanuki et al., 2001). The Sm22-Cre mouse was provided by H. Yanagisawa (University of Texas Southwestern, Dallas, TX). This mouse contains a transgene consisting of a smooth muscle–

specific promoter from the *Tagln (Sm22)* gene and the coding sequence of Cre recombinase (Holtwick et al., 2002).

### Cell culture

HEK293T, U2OS, and HeLa cells were obtained from the American Type Culture Collection. HeLa shRNA stable cells for CCC and retromer components were generated by lentiviral infection of HeLa cells. Viruses were produced using the shRNA expression vector pLKO.TRC, including specific targeting sequences that have been previously reported (Phillips-Krawczak et al., 2015). Mouse *Commd1*-deficient fibroblasts were generated by harvesting *Commd1*$^{f/f}$ embryos at E13.5 and deriving primary MEFs cultures from the embryonic soma. These cultures were immortalized using lentiviral vectors expressing E1A and Ras. Immortalized MEFs were then transiently infected with an adenoviral vector expressing Cre, resulting in *Commd1* deletion, as described previously (Vonk et al., 2011). Dermal fibroblasts from patients with the *CCDC22* p.T17A mutation (Voineagu et al., 2012) were obtained and immortalized through stable expression of telomerase; these cells have been reported previously (Starokadomskyy et al., 2013). MEFs from gene trap and floxed *Commd9* mouse embryos were harvested and immortalized as described here for Commd1-deficient fibroblasts (Vonk et al., 2011). OP9-Jagged1 cells were generated by transduction of the murine bone marrow stromal cell line OP9 with a retroviral vector expressing human Jagged1, as previously reported (Dontje et al., 2006). All cell lines were maintained in high-glucose DMEM containing 10% FBS. Treatment with Bafilomycin A1 (Tocris) consisted of adding this reagent to the growth media (100 nM) for 24 h. Stimulation with plate-bound Jagged1 (R&D Systems) consisted of first applying the ligand to empty growth plates for 24 h (0.5 µg per well of a six-well plate). Thereafter, the plates were rinsed, and cells were seeded onto these plates; 48 h later, RNA was extracted from these cells for analysis. Stimulation with OP9 cells expressing Jagged1 consisted of first seeding the stimulating cells onto plates and allowing them to reach confluency. At that point, cells were rinsed and fixed with sterilized 4% PFA at room temperature for 15 min. After thoroughly rinsing the fixative, target cells were seeded onto these coated plates; 48 h later, RNA was extracted from these cells for analysis.

### Plasmids, RNAi, and CRISPR/Cas9

The pEBB vector is a derivative of pEF-BOS (Mizushima and Nagata, 1990) and contains an EF-1α promoter for mammalian protein expression. A series of derivatives of the pEBB vector (pEBB-HA, pEBB-2xHA-TB, pEBB-HA-COMMD9, and pEBB-2xHA-COMMD9-TB) were generated for these studies through conventional cloning techniques and have been previously described (Starokadomskyy et al., 2013). pEBB-AcGFP1-Rab5c and pEBB-AcGFP1-Rab11b are derivatives of pEBB containing the coding sequence for the fluorescent protein AcGFP1 and the ORFs for Rab5c and Rab11b, respectively. These were cloned into the BamHI and NotI sites of the pEBB-AcGFP1 vector (Phillips-Krawczak et al., 2015). A series of bacterial expression vectors were generated through conventional cloning techniques and include pET30a-His-COMMD1 (expressing His-tagged COMMD1), pGEX-4T1-GST-COMMD6 (expressing GST-tagged COMMD6), pRSF-His-COMMD9 (expressing His-tagged COMMD9), and p15Cool2-MBP-COMMD5 (expressing MBP-tagged COMMD5. The Notch reporter plasmid Notch-CBF1 contains multimerized RBPj binding sites and was shared by L. Lum with permission from the original developers of the construct (Baladrón et al., 2005). The pcDNA-human Notch2FL vector, which expresses full-length untagged Notch2, was provided by Artavanis-Tsakonas Lab (Zagouras et al., 1995). pEBB-2xHA-human Notch2 C terminus (intracellular domain) was PCR amplified from pcDNA-human Notch2FL and cloned into BamHI–NotI sites of pEBB-2xHA vector. For lentiviral expression of HA-tagged COMMD9, we used the lentiviral FG9 vector (Wright and Duckett, 2009). After cloning into the XbaI sites, we generated the FG9-PuroR-HA-COMMD9 vector. A "CRISPR-resistant" version of COMMD9 was introduced into a lentiviral vector (FG9-HygroR-2xHA-Crispr resistant COMMD9) after introducing silent mutations in COMMD9 (site-directed mutagenesis kit; Agilent Technologies) using the following primer: 5′-GCAAGATGGCTGCCCTAACGGCAGAGCATTTTGCAGCAC-3′ (mutated nucleotides are underlined). The siRNA duplexes used in this study are described in Table S2. Stable shRNA-mediated silencing was performed using the lentiviral vector pLKO.TRC. CRISPR-mediated inactivation of COMMD9 was performed through stable expression of a targeting guide RNA (gRNA) and Cas9, using the pLENTI-CRISPR vector (Mali et al., 2013; Shalem et al., 2014). Deleted clones were isolated through limiting dilution and screened for COMMD9 expression by immunoblot. Genomic DNA was isolated from individual clones, and genomic regions around the targeted area were amplified using the following primers: forward (5′-TCTCGGGGTTTAGTCATCCAGCC-3′) and reverse (5′-AGCAGGAGGTTGTATTGCGCCT-3′). These PCR products were cloned into PCR 2.1 TA vector (Life Technologies), and individual clones were sequenced. Nested PCR to obtain a shorter 283-bp product was performed using primers as forward (5′-ACCACAACCGAAACGCCTTCCC-3′) and reverse (5′-AGCAGCAGAGTTGTGGCTCCAA-3′). The resulting amplified products were resolved in 3% Nu-Sieve agarose gels. All targeting sequences used in the various approaches mentioned here are noted in Table S2.

### Transfection and viral transduction

The following transfection reagents were used: calcium phosphate (for plasmids and siRNA in HEK293T cells), Fugene (Roche, for plasmids in U2OS cells), and RNAiMAX (for siRNA in HeLa cells; Life Technologies). Lentiviral production was achieved through transient transfection of HEK293T cells with packaging and expression lentiviral vectors. Culture supernatants containing viral particles were harvested 48 h later, and after filtration through a 0.45-µm filter, this supernatant was applied to the intended cell target. The lentiviral expression vectors used here included puromycin or hygromycin resistance as selection markers, which were used to select stably transduced cells as described previously in more detail (Maine et al., 2007).

### RNA extraction and RT-PCR

RNA extraction from cultured cells was performed using the Trizol method (Life Technologies) according to standard protocols. RNA extraction from isolated embryo hearts was performed using RNeasy columns (QIAGEN). Quantitative RT-PCR was performed using the Sybr green method, and relative quantitation was performed according to the $2^{(-\Delta\Delta Ct)}$ algorithm as previously reported (Maine et al., 2007; Starokadomskyy et al., 2013). The primers used for each of the gene targets examined here are noted in Table S3. All experiments involved biological and technical replicates ($n = 3$) and were performed at least three independent times.

### Protein extraction, immunoblotting, immunoprecipitation, and luciferase assays

Cell lysate preparation, immunoprecipitation, and immunoblotting were performed as previously described (Maine et al., 2007). Immunoblotting and immunoprecipitation experiments were performed using a Triton X-100 lysis buffer (25 mM Hepes, 100 mM NaCl, 10 mM DTT, 1 mM EDTA, 10% glycerol, and 1% Triton X-100). All Western blots presented in this paper are representative of at least three independent iterations for each experiment. Luciferase assays were performed by

transfecting the luciferase reporter plasmid vector (Notch-CBF1) into U2OS cells. After 24 h, the cells were lysed, and 10 µl whole-cell lysate was loaded onto a 96-well luminometer plate. Luciferase substrate (Promega) was injected, and light emission was measured using a luminometer plate reader (EnVision; PerkinElmer), as previously reported (Burstein et al., 2005).

### In vitro binding assay

Bacterial expressing plasmids were individually transformed or cotransformed into to *E. coli* BL21 (DE3) cells (Invitrogen). All cells were grown in LB at 37°C with appropriate antibiotics until OD600 reached 0.6, and they were then shifted to 25°C for at least 30 min. Proteins were expressed at 25°C for 12–16 h by induction with 0.4 mM IPTG. Cells were resuspended in PBS buffer supplied with β-mercaptoethanol and protease inhibitors and lysed by sonication. The lysate was cleared by centrifugation at 12,000 rpm at 4°C for 30 min. For MBP-COMMD5, MBP-COMMD5/His-COMMD1, and MBP-COMMD5/His-COMMD9, clarified supernatant was purified using Amylose resin (NEB). For His-COMMD1/GST-COMMD6, supernatant was purified using glutathione agarose affinity resin (Molecular Probe). After incubation at 4°C for 30 min, the resin was washed four times with PBS buffer. Proteins bound to the resin were eluted with maltose and glutathione.

pEBB-2xHA-Notch2 C terminus was expressed in HEK293T cells, and Notch2-C was immunoprecipitated with HA-affinity beads (Roche). After extensive washing, the protein was eluted from the column with excess HA peptide (Anaspec). GST and His-COMMD1/GST-COMMD6 elution were rebound to glutathione resin. MBP, MBP-COMMD5, and MBP-COMMD5/His-COMMD9 elution were rebound to Amylose resin. The beads bound to these recombinant COMMD complexes were blocked with 5% BSA for 1 h at 4°C. Eluted Notch2-C was then mixed for 1 h at 4°C with COMMD complexes immobilized onto beads. After extensive washing of these beads, the material was resolved by SDS-PAGE and immunoblotted with HA antibody to detect 2xHA-Notch2 C terminus. The SDS-PAGE gels were stained with Coomassie blue.

### Antibodies

All other antibodies used in this study are listed in Table S4. COMMD protein antibodies were generated by immunizing rats (COMMD1, COMMD2, and COMMD3), rabbits (COMMD4, COMMD5, COMMD9, and COMMD10), and guinea pigs (COMMD8) with recombinant GST fusion proteins encoding the N-terminal regions (proximal to the COMM domains) of the respective COMMD proteins (Cocalico Biologicals). The obtained sera were thereafter affinity purified using a $His_6$-tagged version of the respective immunogen (AminoLink Coupling Resin and Immobilization kit; Thermo Fisher Scientific). The antibodies were characterized by testing their ability to recognize FLAG-tagged protein expressed in HEK293 cells without cross reactivity to other COMMDs and to recognize endogenous protein (using siRNA as an additional control). Previously made custom antibodies to COMMD1, COMMD6, and COMMD9 have been reported (Starokadomskyy et al., 2013).

### Immunofluorescence staining

Cell staining was performed as previously reported (Phillips-Krawczak et al., 2015). In brief, cells were seeded in chambered slides and fixed in 4% PFA, permeabilized, and thereafter stained using the specific antibodies indicated in each experiment. The fluorochromes used in the secondary antibodies used for staining were Alexa Fluor 488 and Alexa Fluor 555 (Invitrogen). Images were obtained at room temperature using any of the following confocal microscopes: LSM 510 (63×/1.4 oil immersion objective lens; Carl Zeiss), LSM 710 (63×/1.4 oil immersion objective lens; Carl Zeiss), or A1R (60×/1.4 oil immersion objective lens; Nikon). Images were acquired using LSM 510 (Carl Zeiss), ZEN software (Carl Zeiss), and NIS-Elements AR (Nikon) software, respectively. Obtained images were analyzed using the LSM image browser, ZEN software, or Fuji ImageJ.

### Biotinylation of plasma membrane proteins

Cell-surface biotinylation was performed as previously described (Phillips-Krawczak et al., 2015). In brief, NHSSS-biotin (Pierce) dissolved in biotinylation buffer (10 mM triethanolamine, 150 mM NaCl, and 2 mM $CaCl_2$, pH 8.0) was used for surface labeling at 4°C for 30 min. The biotinylated antigens were precipitated using NeutrAvidin agarose resin (Pierce). Precipitated protein-containing beads were then resuspended in LDS sample buffer (Life Technologies) with 250 mM DTT. Proteins were then subjected to SDS-PAGE, and membranes were probed for Notch2 and N-cadherin.

### Tandem affinity purification

This was performed by sequential purification through HA binding resin (Roche) and Streptavidin agarose (Pierce). In brief, 10 plates of seeded HEK 293 cells (15 cm each) were transfected with pEBB-2xHA-TB or pEBB-2xHA-COMMD9-TB. Two days later, a cell lysate was prepared in Triton X-100 lysis buffer as described in the Protein extraction section. The lysate was incubated with HA binding resin at 4°C for 2 h. At that point, the bait was eluted three times using excess HA peptide (1 mg/ml in 20 mM Tris-HCl, pH 7.4, 100 mM NaCl, and 0.1 mM EDTA). This pooled eluate was applied to a streptavidin agarose beads for 2 h at 4°C. Subsequently, the beads were washed extensively, and proteins were resolved by SDS-PAGE. After Coomassie stain, bands were excised and submitted to the Proteomics core at University of Texas Southwestern for trypsin digestion and peptide identification through LC/MS-MS analysis protein identification. A repeat iteration of this experiment was performed nearly identically except that most of the precipitated material bound to beads was submitted to the Taplin Mass Spectrometry Facility. A small aliquot of the precipitated material was resolved by SDS-PAGE and stained using silver nitrate (Invitrogen).

### Embryological analysis

Timed pregnancies were setup to allow embryo harvesting at specified embryologic stages. Yolk sacs were used as a source of DNA for genotyping. For conventional histologic analysis (HE sections), the embryos were rinsed in PBS and then fixed in 4% PFA in 1× PBS overnight at 4°C with gentle rocking. Thereafter, embryos were dehydrated and stored in 75% ethanol at −20°C. For paraffin embedding, embryos were washed twice in 100% ethanol and xylene for 1 h each, followed by a series of rinses in 100% Paraplast Plus tissue embedding medium (McCormick) at 60°C. Subsequently, these embryos were paraffin embedded, sectioned, and stained according to standard techniques. For immunofluorescence, fixed embryos were rehydrated in stepwise fashion to 1× PBS and rinsed in 30% sucrose overnight at 4°C. The embryos were then embedded in Tissue-Tek O.C.T. compound and sectioned at 10 µm using a cryostat. Antigen retrieval was performed using Buffer A solution (Electron Microscopy Sciences). The slides were washed in 1× PBS and blocked for 1 h in Cas-Block (Invitrogen) before primary antibodies were added for overnight incubation at 4°C. Signals were detected the following day using fluorescently labeled secondary antibodies. The slides were mounted with ProLong Gold Antifade (Invitrogen). Whole-mount in situ hybridization was performed as previously reported (Xu et al., 2009). In brief, the fixed embryos were treated with proteinase K, fixed in a 0.25% glutaraldehyde and 4% PFA solution, and prehybridized at 60°C for 1 h. The samples were transferred into hybridization mix,

containing a digoxigenin-labeled probe. Further in situ hybridization steps were performed with a series of washing buffer, and then development of color reaction was done using BM purple (Roche). RNA probes were generated from the following clones: Apj (BC039224; Open Biosystems) and Cx40 (BC053054; Open Biosystems). Whole-embryo images were obtained with a Stemi 2000-C stereomicroscope (Carl Zeiss) at magnification of 12.5, using a Canon PowerShot G10 camera and AxioVision Rel 4.8 software (Carl Zeiss). In situ staining images were obtained with a NeoLumar Stereomicroscope (Carl Zeiss) with 50×, 75×, or 80× magnification and a DP-70 camera (Olympus) with DP manager software (Olympus). Images of histologic sections were obtained with a DM2000 microscope (Leica) with 4×/0.70, 10×/0.70, 20×/0.70, or 40×/0.75 objective lenses and a Microfire CCD camera (Optronics) with PictureFrame 2.0 software (Optronics).

### Online supplemental material

Fig. S1 shows additional information regarding the CRISPR-targeting strategy used to generated COMMD9-deleted HeLa cell clones (Cr-COMMD9). In addition, characterization of the resulting indels is shown. Fig. S2 shows additional details of the intracellular localization of Notch2 in *COMMD9*-deficient HeLa cells. Fig. S3 displays the effects of CCC or retromer deficiency on Notch2 intracellular localization. Fig. S4 contains details regarding the generation of the two knockout mouse models used here (gene trap and conditional deletion of *Commd9*). Additional morphologic data concerning the phenotype of *Commd9*-deficient embryos are also shown. Fig. S5 shows comparative coimmunoprecipitation of selected COMMD proteins and their associated complexes. Table S1 includes all the hits identified in the tandem affinity purification screen for COMMD9-associated proteins. Table S2 provides sequences for siRNA, shRNA, and CRI SPR reagents used in this paper. Table S3 provides sequences for primers used for quantitative RT-PCR (qRT-PCR). Table S4 includes detailed information for all antibodies used here, including custom-made antibodies against all COMMD proteins which were generated for this study. Online supplemental material is available at http://www.jcb.org/cgi/content/full/jcb.201505108/DC1.


## Acknowledgments

We are grateful to several investigators that provided critical reagents for our studies, including Eric Olson, Rhonda Bassel-Duby (Nkx2.5-Cre mice), Masashi Yanagisawa (Tie2-Cre mice), Hiromi Yanagisawa (Sm22-Cremice), Lawrence Lum (reporter plasmids), and Spyros Artavanis-Tsakonas (Notch2 expression vector). We are also grateful to Eric Olson, Rhonda Basel-Duby, and Doug Engel for their generous help with some of the early embryologic studies. In addition, we are indebted to James Richardson, John Shelton, and the staff of the Molecular Pathology Core for their assistance with several aspects of this study. We are also grateful to the personnel and facilities of the Live Cell Imaging Core at University of Texas Southwestern.

The work of E. Burstein is supported by National Institutes of Health (R01DK073639 and R56AI113274) and CPRIT (RP130409). The work of D.D. Billadeau is supported by National Institutes of Health (grant AI065474). The work of B. van de Sluis is supported by the Netherlands Organization for Scientific Research (NWO-ALW grant 817.02.022).

The authors declare no competing financial interests.

Submitted: 26 May 2015
Accepted: 6 October 2015


## References


Baladrón, V., M.J. Ruiz-Hidalgo, M.L. Nueda, M.J. Díaz-Guerra, J.J. García-Ramírez, E. Bonvini, E. Gubina, and J. Laborda. 2005. dlk acts as a negative regulator of Notch1 activation through interactions with specific EGF-like repeats. *Exp. Cell Res.* 303:343–359. http://dx.doi.org/10.1016/j.yexcr.2004.10.001

Baron, M. 2012. Endocytic routes to Notch activation. *Semin. Cell Dev. Biol.* 23:437–442. http://dx.doi.org/10.1016/j.semcdb.2012.01.008

Biasio, W., T. Chang, C.J. McIntosh, and F.J. McDonald. 2004. Identification of Murr1 as a regulator of the human δ epithelial sodium channel. *J. Biol. Chem.* 279:5429–5434. http://dx.doi.org/10.1074/jbc.M311155200

Burstein, E., J.E. Hoberg, A.S. Wilkinson, J.M. Rumble, R.A. Csomos, C.M. Komarck, G.N. Maine, J.C. Wilkinson, M.W. Mayo, and C.S. Duckett. 2005. COMMD proteins, a novel family of structural and functional homologs of MURR1. *J. Biol. Chem.* 280:22222–22232. http://dx.doi.org/10.1074/jbc.M501928200

Chastagner, P., A. Israël, and C. Brou. 2006. Itch/AIP4 mediates Deltex degradation through the formation of K29-linked polyubiquitin chains. *EMBO Rep.* 7:1147–1153. http://dx.doi.org/10.1038/sj.embor.7400822

Cotton, M., N. Benhra, and R. Le Borgne. 2013. Numb inhibits the recycling of Sanpodo in *Drosophila* sensory organ precursor. *Curr. Biol.* 23:581–587. http://dx.doi.org/10.1016/j.cub.2013.02.020

Couturier, L., K. Mazouni, and F. Schweisguth. 2013. Numb localizes at endosomes and controls the endosomal sorting of notch after asymmetric division in Drosophila. *Curr. Biol.* 23:588–593. http://dx.doi.org/10.1016/j.cub.2013.03.002

Couturier, L., M. Trylinski, K. Mazouni, L. Darnet, and F. Schweisguth. 2014. A fluorescent tagging approach in *Drosophila* reveals late endosomal trafficking of Notch and Sanpodo. *J. Cell Biol.* 207:351–363. http://dx.doi.org/10.1083/jcb.201407071

Derivery, E., C. Sousa, J.J. Gautier, B. Lombard, D. Loew, and A. Gautreau. 2009. The Arp2/3 activator WASH controls the fission of endosomes through a large multiprotein complex. *Dev. Cell.* 17:712–723. http://dx.doi.org/10.1016/j.devcel.2009.09.010

Derivery, E., E. Helfer, V. Henriot, and A. Gautreau. 2012. Actin polymerization controls the organization of WASH domains at the surface of endosomes. *PLoS One.* 7:e39774. http://dx.doi.org/10.1371/journal.pone.0039774

Devlin, A.M., N. Solban, S. Tremblay, J. Gutkowska, W. Schürch, S.N. Orlov, R. Lewanczuk, P. Hamet, and J. Tremblay. 2003. HCaRG is a novel regulator of renal epithelial cell growth and differentiation causing G2M arrest. *Am. J. Physiol. Renal Physiol.* 284:F753–F762. http://dx.doi.org/10.1152/ajprenal.00252.2002

Dontje, W., R. Schotte, T. Cupedo, M. Nagasawa, F. Scheeren, R. Gimeno, H. Spits, and B. Blom. 2006. Delta-like1-induced Notch1 signaling regulates the human plasmacytoid dendritic cell versus T-cell lineage decision through control of GATA-3 and Spi-B. *Blood.* 107:2446–2452. http://dx.doi.org/10.1182/blood-2005-05-2090

Drévillon, L., G. Tanguy, A. Hinzpeter, N. Arous, A. de Becdelièvre, A. Aissat, A. Tarze, M. Goossens, and P. Fanen. 2011. COMMD1-mediated ubiquitination regulates CFTR trafficking. *PLoS One.* 6:e18334. http://dx.doi.org/10.1371/journal.pone.0018334

Fischbach, B.V., K.L. Trout, J. Lewis, C.A. Luis, and M. Sika. 2005. WAGR syndrome: A clinical review of 54 cases. *Pediatrics.* 116:984–988. http://dx.doi.org/10.1542/peds.2004-0467

Fischer, A., N. Schumacher, M. Maier, M. Sendtner, and M. Gessler. 2004. The Notch target genes Hey1 and Hey2 are required for embryonic vascular development. *Genes Dev.* 18:901–911. http://dx.doi.org/10.1101/gad.291004

Fortini, M.E., and D. Bilder. 2009. Endocytic regulation of Notch signaling. *Curr. Opin. Genet. Dev.* 19:323–328. http://dx.doi.org/10.1016/j.gde.2009.04.005

Freeman, C.L., G. Hesketh, and M.N. Seaman. 2014. RME-8 coordinates the activity of the WASH complex with the function of the retromer SNX dimer to control endosomal tubulation. *J. Cell Sci.* 127:2053–2070. http://dx.doi.org/10.1242/jcs.144659

Gomez, T.S., and D.D. Billadeau. 2009. A FAM21-containing WASH complex regulates retromer-dependent sorting. *Dev. Cell.* 17:699–711. http://dx.doi.org/10.1016/j.devcel.2009.09.009

Gomez, T.S., J.A. Gorman, A.A. de Narvajas, A.O. Koenig, and D.D. Billadeau. 2012. Trafficking defects in WASH-knockout fibroblasts originate from collapsed endosomal and lysosomal networks. *Mol. Biol. Cell.* 23:3215–3228. http://dx.doi.org/10.1091/mbc.E12-02-0101

Gridley, T. 2010. Notch signaling in the vasculature. *Curr. Top. Dev. Biol.* 92:277–309. http://dx.doi.org/10.1016/S0070-2153(10)92009-7

Hamada, Y., Y. Kadokawa, M. Okabe, M. Ikawa, J.R. Coleman, and Y. Tsujimoto. 1999. Mutation in ankyrin repeats of the mouse *Notch2* gene induces early embryonic lethality. *Development.* 126:3415–3424.

Harbour, M.E., S.Y. Breusegem, and M.N. Seaman. 2012. Recruitment of the endosomal WASH complex is mediated by the extended 'tail' of Fam21 binding to the retromer protein Vps35. *Biochem. J.* 442:209–220. http://dx.doi.org/10.1042/BJ20111761

Hayashi, S., P. Lewis, L. Pevny, and A.P. McMahon. 2002. Efficient gene modulation in mouse epiblast using a Sox2Cre transgenic mouse strain. *Mech. Dev.* 119(Suppl 1):S97–S101. http://dx.doi.org/10.1016/S0925-4773(03)00099-6

High, F.A., and J.A. Epstein. 2008. The multifaceted role of Notch in cardiac development and disease. *Nat. Rev. Genet.* 9:49–61. http://dx.doi.org/10.1038/nrg2279

Holtwick, R., M. Gotthardt, B. Skryabin, M. Steinmetz, R. Potthast, B. Zetsche, R.E. Hammer, J. Herz, and M. Kuhn. 2002. Smooth muscle-selective deletion of guanylyl cyclase-A prevents the acute but not chronic effects of ANP on blood pressure. *Proc. Natl. Acad. Sci. USA.* 99:7142–7147. http://dx.doi.org/10.1073/pnas.102650499

Hori, K., A. Sen, T. Kirchhausen, and S. Artavanis-Tsakonas. 2011. Synergy between the ESCRT-III complex and Deltex defines a ligand-independent Notch signal. *J. Cell Biol.* 195:1005–1015. http://dx.doi.org/10.1083/jcb.201104146

Hori, K., A. Sen, T. Kirchhausen, and S. Artavanis-Tsakonas. 2012. Regulation of ligand-independent Notch signal through intracellular trafficking. *Commun. Integr. Biol.* 5:374–376. http://dx.doi.org/10.4161/cib.19995

Jia, D., T.S. Gomez, Z. Metlagel, J. Umetani, Z. Otwinowski, M.K. Rosen, and D.D. Billadeau. 2010. WASH and WAVE actin regulators of the Wiskott-Aldrich syndrome protein (WASP) family are controlled by analogous structurally related complexes. *Proc. Natl. Acad. Sci. USA.* 107:10442–10447. http://dx.doi.org/10.1073/pnas.0913293107

Jia, D., T.S. Gomez, D.D. Billadeau, and M.K. Rosen. 2012. Multiple repeat elements within the FAM21 tail link the WASH actin regulatory complex to the retromer. *Mol. Biol. Cell.* 23:2352–2361. http://dx.doi.org/10.1091/mbc.E11-12-1059

Kandachar, V., and F. Roegiers. 2012. Endocytosis and control of Notch signaling. *Curr. Opin. Cell Biol.* 24:534–540. http://dx.doi.org/10.1016/j.ceb.2012.06.006

Kisanuki, Y.Y., R.E. Hammer, J. Miyazaki, S.C. Williams, J.A. Richardson, and M. Yanagisawa. 2001. Tie2-Cre transgenic mice: A new model for endothelial cell-lineage analysis in vivo. *Dev. Biol.* 230:230–242. http://dx.doi.org/10.1006/dbio.2000.0106

Kopan, R. 2012. Notch signaling. *Cold Spring Harb. Perspect. Biol.* 4:a011213. http://dx.doi.org/10.1101/cshperspect.a011213

Lawson, N.D., N. Scheer, V.N. Pham, C.H. Kim, A.B. Chitnis, J.A. Campos-Ortega, and B.M. Weinstein. 2001. Notch signaling is required for arterial-venous differentiation during embryonic vascular development. *Development.* 128:3675–3683.

Liu, Y.F., M. Swart, Y. Ke, K. Ly, and F.J. McDonald. 2013. Functional interaction of COMMD3 and COMMD9 with the epithelial sodium channel. *Am. J. Physiol. Renal Physiol.* 305:F80–F89. http://dx.doi.org/10.1152/ajprenal.00158.2013

Maine, G.N., and E. Burstein. 2007. COMMD proteins: COMMing to the scene. *Cell. Mol. Life Sci.* 64:1997–2005. http://dx.doi.org/10.1007/s00018-007-7078-y

Maine, G.N., X. Mao, C.M. Komarck, and E. Burstein. 2007. COMMD1 promotes the ubiquitination of NF-kappaB subunits through a cullin-containing ubiquitin ligase. *EMBO J.* 26:436–447. http://dx.doi.org/10.1038/sj.emboj.7601489

Mali, P., L. Yang, K.M. Esvelt, J. Aach, M. Guell, J.E. DiCarlo, J.E. Norville, and G.M. Church. 2013. RNA-guided human genome engineering via Cas9. *Science.* 339:823–826. http://dx.doi.org/10.1126/science.1232033

McCright, B., J. Lozier, and T. Gridley. 2006. Generation of new Notch2 mutant alleles. *Genesis.* 44:29–33. http://dx.doi.org/10.1002/gene.20181

McFadden, D.G., A.C. Barbosa, J.A. Richardson, M.D. Schneider, D. Srivastava, and E.N. Olson. 2005. The Hand1 and Hand2 transcription factors regulate expansion of the embryonic cardiac ventricles in a gene dosage-dependent manner. *Development.* 132:189–201. http://dx.doi.org/10.1242/dev.01562

McGill, M.A., S.E. Dho, G. Weinmaster, and C.J. McGlade. 2009. Numb regulates post-endocytic trafficking and degradation of Notch1. *J. Biol. Chem.* 284:26427–26438. http://dx.doi.org/10.1074/jbc.M109.014845

Mizushima, S., and S. Nagata. 1990. pEF-BOS, a powerful mammalian expression vector. *Nucleic Acids Res.* 18:5322. http://dx.doi.org/10.1093/nar/18.17.5322

Phillips-Krawczak, C.A., A. Singla, P. Starokadomskyy, Z. Deng, D.G. Osborne, H. Li, C.J. Dick, T.S. Gomez, M. Koenecke, J.S. Zhang, et al. 2015. COMMD1 is linked to the WASH complex and regulates endosomal trafficking of the copper transporter ATP7A. *Mol. Biol. Cell.* 26:91–103. http://dx.doi.org/10.1091/mbc.E14-06-1073

Reichardt, I., and J.A. Knoblich. 2013. Cell biology: Notch recycling is numbed. *Curr. Biol.* 23:R270–R272. http://dx.doi.org/10.1016/j.cub.2013.03.013

Rottner, K., J. Hänisch, and K.G. Campellone. 2010. WASH, WHAMM and JMY: Regulation of Arp2/3 complex and beyond. *Trends Cell Biol.* 20:650–661. http://dx.doi.org/10.1016/j.tcb.2010.08.014

Sakata, T., H. Sakaguchi, L. Tsuda, A. Higashitani, T. Aigaki, K. Matsuno, and S. Hayashi. 2004. Drosophila Nedd4 regulates endocytosis of notch and suppresses its ligand-independent activation. *Curr. Biol.* 14:2228–2236. http://dx.doi.org/10.1016/j.cub.2004.12.028

Seaman, M.N., A. Gautreau, and D.D. Billadeau. 2013. Retromer-mediated endosomal protein sorting: All WASHed up! *Trends Cell Biol.* 23:522–528. http://dx.doi.org/10.1016/j.tcb.2013.04.010

Shalem, O., N.E. Sanjana, E. Hartenian, X. Shi, D.A. Scott, T.S. Mikkelsen, D. Heckl, B.L. Ebert, D.E. Root, J.G. Doench, and F. Zhang. 2014. Genome-scale CRISPR-Cas9 knockout screening in human cells. *Science.* 343:84–87. http://dx.doi.org/10.1126/science.1247005

Smith, L., P. Litman, and C.M. Liedtke. 2013. COMMD1 interacts with the COOH terminus of NKCC1 in Calu-3 airway epithelial cells to modulate NKCC1 ubiquitination. *Am. J. Physiol. Cell Physiol.* 305:C133–C146. http://dx.doi.org/10.1152/ajpcell.00394.2012

Starokadomskyy, P., N. Gluck, H. Li, B. Chen, M. Wallis, G.N. Maine, X. Mao, I.W. Zaidi, M.Y. Hein, F.J. McDonald, et al. 2013. CCDC22 deficiency in humans blunts activation of proinflammatory NF-κB signaling. *J. Clin. Invest.* 123:2244–2256. http://dx.doi.org/10.1172/JCI66466

Steinberg, F., M. Gallon, M. Winfield, E.C. Thomas, A.J. Bell, K.J. Heesom, J.M. Tavaré, and P.J. Cullen. 2013. A global analysis of SNX27-retromer assembly and cargo specificity reveals a function in glucose and metal ion transport. *Nat. Cell Biol.* 15:461–471. http://dx.doi.org/10.1038/ncb2721

Tao, T.Y., F. Liu, L. Klomp, C. Wijmenga, and J.D. Gitlin. 2003. The copper toxicosis gene product Murr1 directly interacts with the Wilson disease protein. *J. Biol. Chem.* 278:41593–41596. http://dx.doi.org/10.1074/jbc.C300391200

Troost, T., S. Jaeckel, N. Ohlenhard, and T. Klein. 2012. The tumour suppressor Lethal (2) giant discs is required for the function of the ESCRT-III component Shrub/CHMP4. *J. Cell Sci.* 125:763–776. http://dx.doi.org/10.1242/jcs.097261

van de Sluis, B., J. Rothuizen, P.L. Pearson, B.A. van Oost, and C. Wijmenga. 2002. Identification of a new copper metabolism gene by positional cloning in a purebred dog population. *Hum. Mol. Genet.* 11:165–173. http://dx.doi.org/10.1093/hmg/11.2.165

van de Sluis, B., P. Muller, K. Duran, A. Chen, A.J. Groot, L.W. Klomp, P.P. Liu, and C. Wijmenga. 2007. Increased activity of hypoxia-inducible factor 1 is associated with early embryonic lethality in *Commd1* null mice. *Mol. Cell. Biol.* 27:4142–4156. http://dx.doi.org/10.1128/MCB.01932-06

van de Sluis, B., X. Mao, Y. Zhai, A.J. Groot, J.F. Vermeulen, E. van der Wall, P.J. van Diest, M.H. Hofker, C. Wijmenga, L.W. Klomp, et al. 2010. COMMD1 disrupts HIF-1α/β dimerization and inhibits human tumor cell invasion. *J. Clin. Invest.* 120:2119–2130. http://dx.doi.org/10.1172/JCI40583

Voineagu, I., L. Huang, K. Winden, M. Lazaro, E. Haan, J. Nelson, J. McGaughran, L.S. Nguyen, K. Friend, A. Hackett, et al. 2012. CCDC22: A novel candidate gene for syndromic X-linked intellectual disability. *Mol. Psychiatry.* 17:4–7. http://dx.doi.org/10.1038/mp.2011.95

Vonk, W.I., P. Bartuzi, P. de Bie, N. Kloosterhuis, C.G. Wichers, R. Berger, S. Haywood, L.W. Klomp, C. Wijmenga, and B. van de Sluis. 2011. Liver-specific *Commd1* knockout mice are susceptible to hepatic copper accumulation. *PLoS One.* 6:e29183. http://dx.doi.org/10.1371/journal.pone.0029183

Wang, Q., N. Zhao, S. Kennard, and B. Lilly. 2012. Notch2 and Notch3 function together to regulate vascular smooth muscle development. *PLoS One.* 7:e37365. http://dx.doi.org/10.1371/journal.pone.0037365

Wilkin, M., P. Tongngok, N. Gensch, S. Clemence, M. Motoki, K. Yamada, K. Hori, M. Taniguchi-Kanai, E. Franklin, K. Matsuno, and M. Baron. 2008. *Drosophila* HOPS and AP-3 complex genes are required for a Deltex-regulated activation of notch in the endosomal trafficking pathway. *Dev. Cell.* 15:762–772. http://dx.doi.org/10.1016/j.devcel.2008.09.002

Wilkin, M.B., A.M. Carbery, M. Fostier, H. Aslam, S.L. Mazaleyrat, J. Higgs, A. Myat, D.A. Evans, M. Cornell, and M. Baron. 2004. Regulation of notch endosomal sorting and signaling by *Drosophila* Nedd4 family proteins. *Curr. Biol.* 14:2237–2244. http://dx.doi.org/10.1016/j.cub.2004.11.030

Wright, C.W., and C.S. Duckett. 2009. The aryl hydrocarbon nuclear translocator alters CD30-mediated NF-kappaB-dependent transcription. *Science*. 323:251–255. http://dx.doi.org/10.1126/science.1162818

Xu, K., D.C. Chong, S.A. Rankin, A.M. Zorn, and O. Cleaver. 2009. Rasip1 is required for endothelial cell motility, angiogenesis and vessel formation. *Dev. Biol.* 329:269–279. http://dx.doi.org/10.1016/j.ydbio.2009.02.033

Xu, S., J.C. Han, A. Morales, C.M. Menzie, K. Williams, and Y.S. Fan. 2008. Characterization of 11p14-p12 deletion in WAGR syndrome by array CGH for identifying genes contributing to mental retardation and autism. *Cytogenet. Genome Res.* 122:181–187. http://dx.doi.org/10.1159/000172086

Zagouras, P., S. Stifani, C.M. Blaumueller, M.L. Carcangiu, and S. Artavanis-Tsakonas. 1995. Alterations in Notch signaling in neoplastic lesions of the human cervix. *Proc. Natl. Acad. Sci. USA*. 92:6414–6418. http://dx.doi.org/10.1073/pnas.92.14.6414

Zheng, L., P. Liang, J. Li, X.B. Huang, S.C. Liu, H.Z. Zhao, K.Q. Han, and Z. Wang. 2012. ShRNA-targeted COMMD7 suppresses hepatocellular carcinoma growth. *PLoS One.* 7:e45412. http://dx.doi.org/10.1371/journal.pone.0045412